Effects of geometric and electronic structure on the finite temperature behavior of Na$_{58}$, Na$_{57}$, and Na$_{55}$ cluster

Mal-Soon Lee[*] and D. G. Kanhere[†]

Centre for Modeling and Simulation, and Department of Physics, University of Pune, Ganeshkhind, Pune 411 007, India
(Received 31 July 2006; revised manuscript received 28 December 2006; published 26 March 2007)

We report the equilibrium geometries and the electronic structures of Na$_n$ clusters in the size range of n = 55–62 using density-functional method. An analysis of the evolutionary trends in their ground state geometries reveals that Na$_{58}$ has a spherical shape which is driven by the closed-shell nature of the electronic structure. This structure shows a significant large network connected by short bonds among the surface atoms as well as between core and surface atoms, which affects its finite-temperature behavior. By employing *ab initio* density-functional molecular dynamics, we calculate the specific heat of Na$_{58}$ and Na$_{57}$. We observe two distinct features in their specific-heat curves as compared to that of Na$_{55}$: (1) Both clusters show very broad melting transition. (2) The calculated melting temperature of Na$_{58}$ is ~375 K, the highest one studied so far, and that of Na$_{57}$ is also relatively high (~350 K). Thus, when a cluster has a (nearly) geometric closed-shell structure as well as a (nearly) electronic closed-shell one, it shows a high melting temperature. Our calculations clearly bring out the size-sensitive nature of the specific-heat curve in sodium clusters.

I. INTRODUCTION

The finite-temperature behavior of sodium clusters has attracted much attention since the pioneering experimental work by Haberland and co-workers.[1,2] These experiments reported melting temperatures of sodium clusters in the size range of 55 to 350 atoms. A great deal of effort has been spent to understand and explain the main puzzling feature, namely the irregular variation in the observed melting points. Equally puzzling is the observation that Na$_{57}$ and Na$_{142}$, which is neither geometric shell-closing systems nor electronic shell-closing systems, show higher melting temperatures than the vicinity systems such as Na$_{55}$, Na$_{138}$, and Na$_{147}$. It is interesting to note that Na$_{55}$ and Na$_{147}$ are geometric shell-closing clusters and Na$_{138}$ is an electronic shell-closing one. Although it is expected that there is an intricate interplay between the electronic and geometric structures so far as finite temperature behavior is concerned, the consensus seems to be that the geometry dominates the melting characteristics and the effects of electronic structure are secondary.[2,3] This has been a surprise since the stability of these clusters is almost entirely dictated by the electronic structure.

Recently a very different aspect of the finite-temperature behavior has been revealed in the experimental measurements of heat capacities of gallium and aluminum clusters,[4] namely the size-sensitive nature of their *shapes*. A definitive correlation between the shape of specific-heat curve and the nature of the ground-state geometry in gallium cluster has also been established by our group.[5] Surprisingly, in spite of extensive work reported on the benchmark system of sodium clusters, there is no report of such a size sensitivity.

Motivated by the above observations, we have carried out extensive density-functional calculations to analyze the growth pattern of the clusters in the size range from 55 to 62. In addition, we report the specific-heat curves of Na$_{58}$ and Na$_{57}$ obtained by *ab initio* density-functional molecular dynamics simulations. In particular, we examine the relation-ship between the geometry and the shape of the specific-heat curve, and between the electronic structure and the melting temperature. It is interesting to note that there are very few cases in sodium clusters where an electronic shell-closing system (n = 8, 20, 40, 58, 138, …) has a similar size as a geometric shell-closing one (n = 55, 147, 309, …). For instance, a pair of clusters n = 55 and n = 58 differs by three atoms only. Another example is a pair {n = 138 and 147} having nine-atom difference. The next such occurrence is at n = 309 and n = 338, which is not close enough. Therefore, the expected effects due to both the geometric and electronic magic numbers are likely to be seen prominently in {55, 58} range. The electronically closed-shell structure of Na$_{58}$ and nearly electronic shell-closing system of Na$_{57}$ have slightly distorted icosahedral structures as their ground-state geometries compared to the geometric shell-closing cluster of Na$_{55}$. Indeed, as we shall see, Na$_{58}$ and Na$_{57}$ have significantly different finite-temperature characteristics as compared to those of geometrically closed-shell cluster, Na$_{55}$. First, the shape of the specific-heat curve is much broader than that of Na$_{55}$. Second, they show peaks (rather broad) at the temperature approximately 375 K for Na$_{58}$ and 350 K for Na$_{57}$. We note that the observed melting temperature of Na$_{57}$ by Haberland and co-workers[1] is about 325 K which differs less than 8% from our result. Specially, in case of Na$_{58}$ this is the first observation that a melting temperature of sodium cluster can be closed to that of the bulk. Interestingly, it is observed that Na$_{58}$ shows high abundance in mass spectra, indicating its high stability.[1]

The paper is organized as follows: in Sec. II, we briefly mention computational details used. In Sec. III we discuss our results, and summarize the results in Sec. IV.

II. COMPUTATIONAL DETAILS

We have carried out Born-Oppenheimer molecular-dynamics simulations using ultrasoft pseudopotentials within

the local-density approximation (LDA).[6] In order to get an insight into the evolutionary pattern of the geometries, we have obtained equilibrium structures for Na_n (n=55 to 62). Our thorough search of the lowest-energy structure is performed by obtaining at least 180 distinguishable equilibrium configurations for each of the clusters by using a combination of a basin-hopping algorithm and density-functional methods. We have carried out extensive *ab initio* constant-temperature simulations using a Nose-Hoover thermostat for Na_{58} and Na_{57}. These simulations have been carried out at 16 temperatures for Na_{58} and at 12 temperatures for Na_{57} in the range of 80 K ≤ T ≤ 500 K for the period of at least 210 ps (240 ps near the melting temperature), total simulation times of 3.5 ns and 2.7 ns, respectively. Our cell size used is $24 \times 24 \times 24$ Å^3, with the energy cutoff of 3.6 Ry whose reliability has been examined in our previous work.[7] We use the multiple-histogram technique to calculate the canonical specific heat, defined as

$$C = \frac{\partial U}{\partial T},$$

where $U = \langle V+K \rangle_T$ is the average total internal energy in a canonical ensemble at temperature T. Since we exclude the contribution of the center-of-mass motion to the ionic kinetic energy K, we only have internal rotational and vibrational degrees of freedom. Thus,

$$\langle K \rangle_T = \tfrac{1}{2}(3N-3)k_B T,$$

with N being the number of atoms in the cluster. At sufficiently low T, in addition, since the ions show simple harmonic motion, the potential energy contains the vibrational degrees of freedom ($3N-6$). Thus, at low T,

$$\langle V \rangle_T \approx \tfrac{1}{2}(3N-6)k_B T.$$

Combining three above equations, one obtains the zero-temperature classical limit of the rotational plus vibrational specific heat such as

$$C_0 = (3N-9/2)k_B,$$

which is conveniently used to normalize our plots of canonical specific heat. More details of the methods can be found in Ref. 8. For the analysis, we have taken the last 165 ps data from each temperature, leaving at least the first 45 ps for thermalization. The data for Na_{55} is taken from Ref. 7. The reliability of our calculation can be judged from the fact that our earlier calculations based on density-functional theory (DFT) (Ref. 7) have successfully reproduced the experimental melting temperatures of Na_n (n=55, 92, and 142).[2]

III. RESULTS AND DISCUSSION

The lowest-energy structures of Na_n (n=55–62) are shown in Fig. 1. There are some striking features evident in their evolutionary pattern. The ground-state geometry (GS) of Na_{55} is the well-known icosahedron.[9] A single extra atom added to Na_{55} is accommodated on the surface by a minor adjustment of surface atoms. When the second atom is added, it is energetically more favorable to retain the icosa-
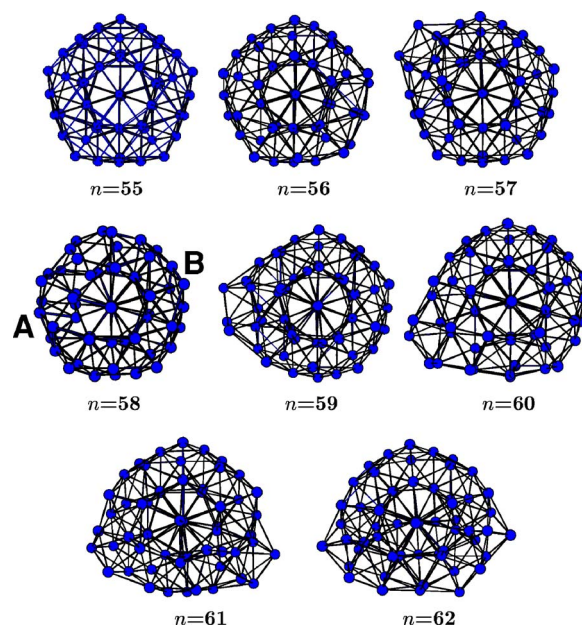

FIG. 1. (Color online) The ground-state geometry of Na_n (n=55–62). In the figure of Na_{58}, "A" indicates the region where three extra atoms are accommodated compared to Na_{55}, and "B" indicates the region where the geometry of Na_{55} is retained.

hedral core with two atoms *capping* it. Very interestingly, when three atoms are added (n=58), instead of the pattern of capping continuing, all three atoms are accommodated on the surface of icosahedron, making the structure again nearly spherical without changing the size of Na_{55} significantly. This can be verified by examining the distance from the center of mass (C.O.M.). In Fig. 2, we show the distances from C.O.M. for each atom in Na_{58} and Na_{59}. For the comparison the data for Na_{55} is also seen. The radial shell structure in the case of Na_{58} is evident. However, the distribution of atoms in Na_{59} is comparatively different than seen in Na_{55}. The pattern of growth from Na_{59} to Na_{62} changes back to the capping mode as can be seen in Fig. 1. This peculiar shape transformation observed in Na_{58} can be examined by plotting deformation parameter ε_{def}. ε_{def} is defined as $\varepsilon_{\text{def}} = 2Q_1/(Q_2+Q_3)$, where $Q_1 \geq Q_2 \geq Q_3$ are eigenvalues of the quadrupole
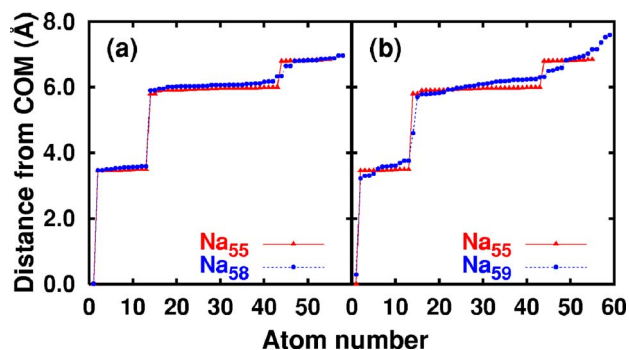

FIG. 2. (Color online) The distance from the center of mass of each atom in Na_{58} and Na_{59} in comparison with that of Na_{55}. In Na_{58} the maximum distance is almost the same as seen in Na_{55}, while that in Na_{59} is changed significantly.
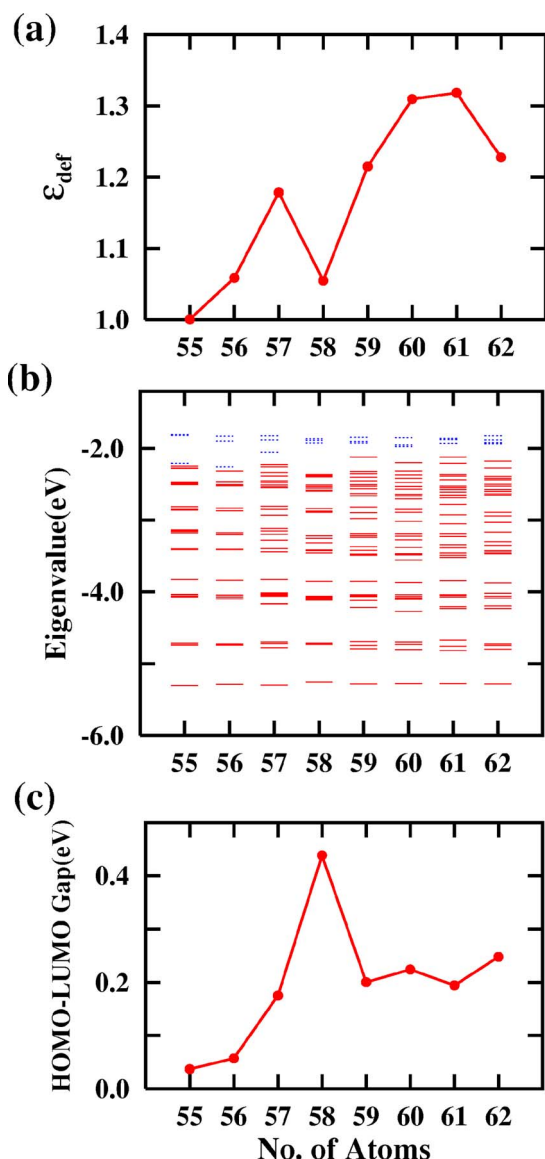
FIG. 4. (Color online) The histogram of bond lengths for the ground-state geometry of Na_{58}, Na_{57}, and Na_{55}, with less than that of the bulk (3.71 Å).

present studied systems [Fig. 3(c)]. Thus, an electronically closed-shell nature of Na_{58} results into a spherical charge density distribution which drives the geometry towards a spherical shape. Our calculations bring out the fact that this change of shape induces the GS geometry to be compact with a significant structural disorder in Na_{58}. This is an example of an *electronically driven shape change*.

A strong correlation between the nature of the bonding in the GS geometry and the shape of the specific-heat curve has been established in the case of Ga clusters.[5,10] Therefore, we analyze the geometries by examining the number of the short bonds and how they are connected in the cluster (we call this "*connectivity*"). Figure 4 shows the number of bonds having bond lengths less than 3.71 Å, the bulk bond length, for Na_{58} and Na_{57} along with that in Na_{55} as histogram. It turns out that Na_{58} has 21 bonds shorter than the shortest bond in Na_{55}. Further, all of these bonds are located in the region A shown in Fig. 1, giving rise to an island of relatively strongly bonded atoms as compared to Na_{55}. In Na_{57} there are 16 bonds which are shorter than the shortest bond in Na_{55}. In order to bring out the difference in the connectivity of the short bonds, we show the connectivity for different bonds having bond lengths less than 3.45 Å [Figs. 5(a)–5(c)] and less than 3.55 Å [Figs. 5(d)–5(f)]. The significant difference between the regions A and B (also see Fig. 1) in Na_{58} is clear [Fig. 5(a)]. The majority of the strongly bonded atoms in Na_{58} forms a connected island in the region A, while all the short bonds in Na_{55} are radial [Fig. 5(c)]. A comparison of Fig. 5(d) and Fig. 5(f) brings out another significant difference in Na_{58} and Na_{55}. In Na_{55} the connectivity is established only between the core (first shell) and the surface atoms, while in addition the surface atoms are also connected to each other in Na_{58}. The connectivity seen in Na_{57} [Fig. 5(b) and Fig. 5(e)] is intermediate between these two cases, but it is closer to those of Na_{58}. Thus, it can be seen that to accommodate three extra atoms over Na_{55}, distances between the first shell and the surface atoms are reduced, resulting in a strong network extending over the entire cluster with inhomogeneous strength. In a recent work, Aguado and López[3] have attributed the higher melting temperature seen in the experiments on sodium clusters,[1,2] to the existence of short bonds between the surface and first-shell atoms. Our calculations are consistent with their observation.

FIG. 3. (Color online) The comparison of (a) the deformation parameter, ε_{def}, (b) the eigenvalue spectra of the ground-state geometries as a function of cluster size, where solid lines show the occupied orbitals and dotted shorter lines show the unoccupied ones. (c) The HOMO-LUMO gap as a function of cluster size.

tensor $Q_{ij} = \Sigma_I R_{Ii} R_{Ij}$ with R_{Ii} being ith coordinate of ion I relative to the center of mass of the cluster. For a spherical shape $(Q_1 = Q_2 = Q_3)$ ε_{def} is 1.0, while $\varepsilon_{def} > 1.0$ indicates a deformation. It can be seen in Fig. 3(a) that the addition of three atoms over Na_{55} changes the shape to nearly spherical. Interestingly, this difference is also reflected in their eigenvalue spectrum as shown in Fig. 3(b). Although Na_{58} is not as symmetric as icosahedral structure of Na_{55}, rather in the sense of amorphous, it follows jelliumlike pattern very closely in contrast to Na_{57}, Na_{59} to Na_{62} where additional states appear in the gaps due to their disordered structures. Such an effect is absent in Na_{58}. In addition an electronic shell-closing system of Na_{58} shows the largest gap (0.44 eV) between the highest occupied molecular orbital (HOMO) and the lowest unoccupied molecular orbital (LUMO) among the
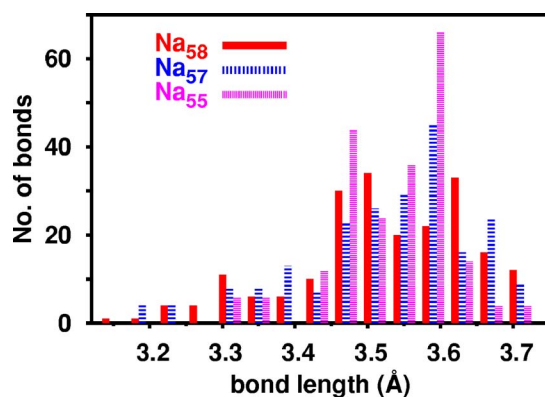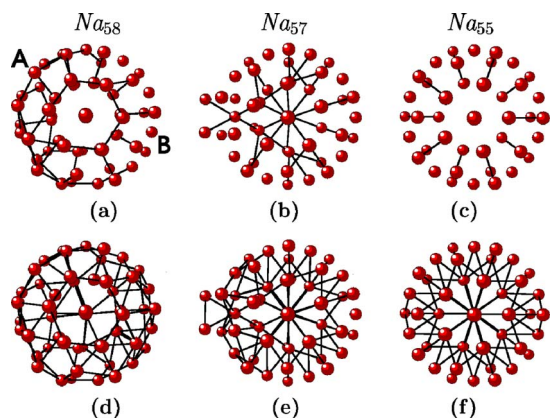
FIG. 5. (Color online) The short-bond connectivity with bond length less than 3.45 Å in (a) Na$_{58}$, (b) Na$_{57}$, (c) Na$_{55}$, showing inhomogeneous distribution of bond strength in Na$_{58}$ and Na$_{57}$. The short-bond connectivity with bond length less than 3.55 Å in (d) Na$_{58}$, (e) Na$_{57}$, (f) Na$_{55}$, showing Na$_{58}$ has strongest connectivity through the entire system among three clusters. In (a), "*A*" and "*B*" indicate the same region as shown in Fig. 1.

We have also analyzed the nature of bonding via the electron localization function (ELF). The ELF (Ref. 11) is defined as

$$\chi_{\text{ELF}} = \left[1 + \left(\frac{D}{D_h} \right)^2 \right]^{-1},$$

where

$$D = \frac{1}{2} \sum_i |\nabla \psi_i|^2 - \frac{1}{8} \frac{|\nabla \rho|^2}{\rho},$$

$$D_h = \frac{3}{10} (3\pi^2)^{5/3} \rho^{5/3}.$$

Here $\rho \equiv \rho(\mathbf{r})$ is the valence electron density and ψ_i's are the KS orbitals. The χ_{ELF} is 1.0 for perfect localized function and 0.5 for plain waves. In Fig. 6, we show the ELF isosurface of Na$_{58}$ for isovalue of $\chi_{\text{ELF}}=0.79$ in two different regions. Figures 6(a) and 6(b) depicts the ELF at 0.79 in regions *A* and *B*, respectively. The contrast is evident. In region *A* which consists of atoms connected by shorter bonds, the ELF isosurface forms a connected network showing the existence of a strongly bonded region containing at least 20 atoms. In contrast, in region *B* such a network is absent. In fact, the region *B* gets connected at a lower isovalue of 0.74. The same analysis has been carried out for N$_{57}$ and Na$_{55}$. Na$_{57}$ shows similar characteristics compared to those seen in Na$_{58}$. A region near the capping atoms [left-hand side in Fig. 5(b)] starts connecting at $\chi_{\text{ELF}}=0.78$, whereas a region away from them is connected at 0.74. The connection of isosurface is established over the entire cluster of Na$_{55}$ at the isovalue of 0.72. Thus, our ELF analysis clearly brings out the existence of strongly bonded island of atoms and the inhomogeneous distribution of bond strength in Na$_{58}$ and Na$_{57}$.

Our study reveals two unique features in the ground-state geometries of Na$_{58}$ and Na$_{57}$. First, the (nearly) electronic shell-closing system induces shortening of bonds, resulting in a strong connectivity of short bonds among the surface
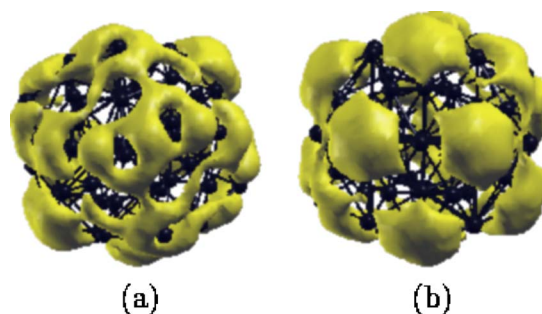

FIG. 6. (Color online) The isovalued surfaces of the electron localization function at $\chi_{\text{ELF}}=0.79$ for Na$_{58}$ (a) in region *A* and (b) in region *B* shown in Fig. 1. The similar pattern of (b) is also seen at $\chi_{\text{ELF}}=0.76$ in Na$_{55}$.

atoms as well as between first-shell and surface atoms compared to only first-shell to core connectivity established in Na$_{55}$. Second, its ground-state geometry is considerably disordered, resulting in inhomogeneous distribution of bond strength as compared to the highly symmetric Na$_{55}$. We argue that these two effects will be manifested in the specific heat differently. The existence of the well connected short bonds are expected to raise the melting temperature as compared to that of Na$_{55}$. The effect of geometric disorder is to broaden the specific heat.

We show the calculated specific-heat curves for Na$_{58}$ and Na$_{57}$ along with those of Na$_{55}$,[7] in Fig. 7. The most symmetric cluster Na$_{55}$ shows a sharp melting transition at 280 K, while the highest melting temperature is seen in Na$_{58}$. Thus, the addition of two or three atoms changes the specific-heat curve drastically. Our calculations clearly demonstrate a strong correlation between the nature of order or lack of order in the GS geometry and their finite temperature behav-
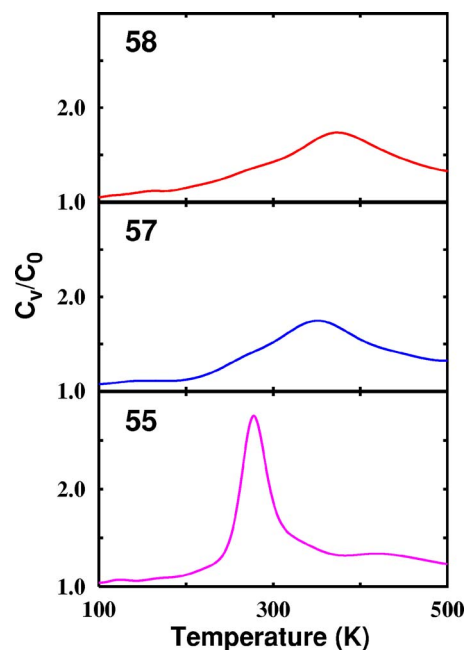

FIG. 7. (Color online) The normalized specific heat as a function of temperature. $C_0=(3N-9/2)k_B$ is the zero-temperature classical limit of the rotational plus vibrational canonical specific heat.
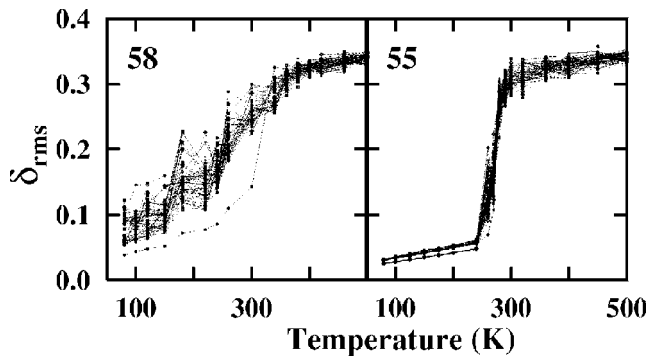
FIG. 8. The comparison of the root-mean-square bond length fluctuation (δ_{rms}) of individual atoms for Na$_{58}$ and Na$_{55}$.

FIG. 9. The comparison of the mean-square displacement (MSD) of individual atoms at 240 K for Na$_{58}$ and Na$_{55}$.

ior, and between the connectivity of short bonds and its melting temperature. This explanation can be extended to the finite temperature behavior in Na$_{50}$ (figure not shown). Na$_{50}$ has a disordered GS geometry but does not possess a strongly connected network.[12] The specific-heat curve of Na$_{50}$, indeed, shows a very broad melting transition with low melting temperature (225 K). The results of the density-functional simulations carried by Rytkönen *et al.*[13] as well as Lee *et al.*[12] are also consistent with the features that emerge out of our present calculation. An electronically closed-shell system Na$_{40}$ has a disturbed spherical GS geometry with a well-connected network of short bonds from core to surface atoms, which is stronger than that of Na$_{55}$. Its specific heat is broader but melting point is higher than that of Na$_{55}$ (figure not shown). Thus, it also brings out the size-sensitive nature of specific-heat curve in sodium clusters, not reported so far either experimentally or computationally. It may be noted that extreme size sensitivity of this kind has been observed experimentally in Ga and Al clusters.[4] We have also calculated the latent heats per atom by using caloric curves. They are estimated as 0.02 eV/atom for Na$_{58}$, 0.016 eV for Na$_{57}$, and 0.014 eV/atom for Na$_{55}$. The latent heats observed by experiment[1] are 0.008 eV/atom for Na$_{57}$ and 0.015 eV/atom for Na$_{55}$. The deviation observed in Na$_{57}$ may be due to its very broad melting transition.

Due to the disordered nature of the GS geometry in Na$_{58}$, we expect different atoms to move with various amplitudes at a given temperature (Fig. 8). To see this, we have calculated the Lindemann criteria, i.e., the root-mean-square bond length fluctuation (δ_{rms}) for individual atoms of Na$_{58}$, where $\delta_{rms}(i)$ for atom i is defined as

$$\delta_{rms}(i) = \frac{1}{N} \sum_j \frac{\sqrt{\langle R_{ij}^2 \rangle_t - \langle R_{ij} \rangle_t^2}}{\langle R_{ij} \rangle_t},$$

where R_{ij} is the distance between i and j ions with $i \neq j$, $N = n-1$ with n be number of atoms in the cluster, and $\langle \cdots \rangle_t$ denotes a time average over the entire trajectory. Indeed, $\delta_{rms}(i)$ in Na$_{58}$ has a broad range of values at a given temperature showing a different response for each atom, while for Na$_{55}$ (highly symmetric structure) they are collective, leading to a sharp transition region. Further, it saturates at nearly 375 K in Na$_{58}$ compared to 280 K in Na$_{55}$. Interest-
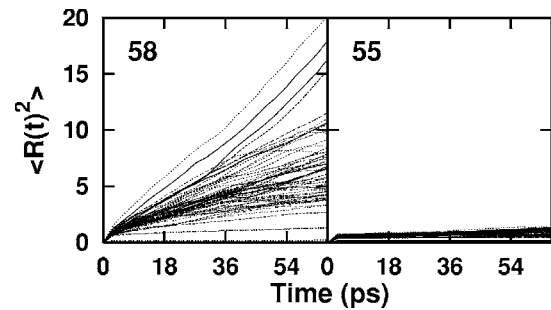
ingly, the center atom in Na$_{58}$ (the bottom most line) dose not develop its melting behavior until 300 K. The disordered nature of the geometry leading to inhomogeneous distribution of bond strength results in distinctly different response of different atoms upon heating. We show the mean-square-displacement (MSD) of individual atoms at 240 K in Fig. 9. Evidently the atoms in these two clusters respond differently when heated. While Na$_{55}$ shows a clear solidlike behavior, a significant number of atoms in Na$_{58}$ show diffusive motion. We also observed the similar characteristics in Na$_{57}$, seen in δ_{rms} and MSD of Na$_{58}$.

In Fig. 10 we show the time-averaged eigenvalues (average over the entire simulation runs) as a function of temperature. Evidently, we do not find the eigenvalue spectra of liquidlike and solidlike systems to be similar. Instead, the HOMO-LUMO gaps in all the cases are closed. According to the calculations of ε_{def} as a function of temperature, after melting their geometries become elongated in these clusters. This can explain the close of the HOMO-LUMO gap. Thus, the present extensive simulations clearly bring out the impor-
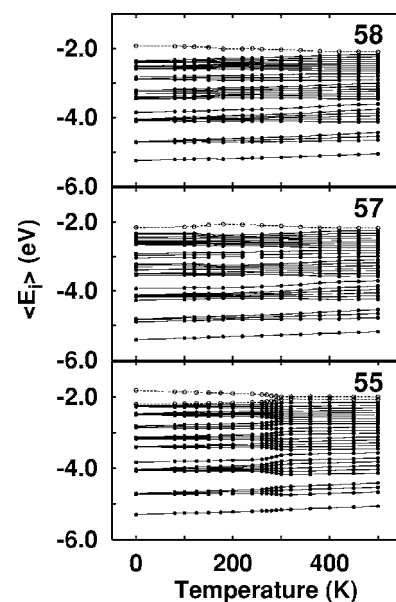

FIG. 10. The averaged eigenvalues of Na$_{58}$, Na$_{57}$, and Na$_{55}$ as a function of temperature. The solid lines show the change of the eigenvalues for the occupied orbitals and dotted lines show that for the unoccupied orbitals.
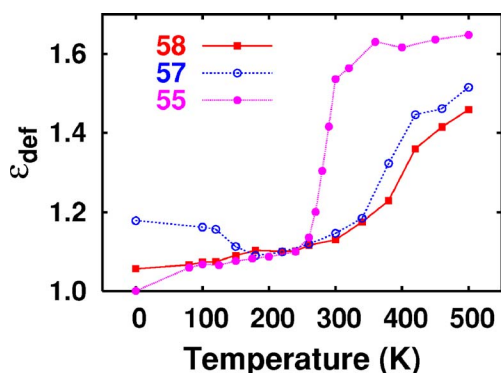
FIG. 11. (Color online) The average deformation parameter of Na_{58}, Na_{57}, and Na_{55} as a function of temperature.

tance and significance of the electronic structure. Interestingly, the change of eigenvalue spectrum and ε_{def} as a function of temperature in Na_{58} and Na_{57} becomes similar after 180 K. Even though the GS geometry of Na_{57} is not spherical, its structure changes towards spherical shape upon heating. Thus, when a cluster has both characteristics of (nearly) closed shell not only geometrically but also electronically, it has high melting temperature compared to those having either geometric close shell or electronic closed shell. It is interesting to note that Na_{58} is observed to have a relatively high abundance in mass spectra. This may explain the reason why Na_{142} has higher melting temperature than Na_{138}, an electronic closed-shell cluster and Na_{147}, a geometric closed-shell one.

IV. SUMMARY

To summarize, the present work brings out the effect of the electronic as well as the geometric structures on the melting of Na_{58} and Na_{57} clusters compared with that of Na_{55} (Fig. 11). The electronic shell-closing nature of Na_{58} drives the GS geometry to be spherical, which leads to a compact and disordered structure. As consequence, in Na_{58} the first shell and surface as well as atoms on the surface are well connected with short bonds. This leads to the high melting temperature of nearly bulk melting temperature. The disordered nature of the system is responsible for rather broad specific-heat curve. Another example of strong connectivity is seen in the GS geometry of Na_{57}, nearly electronic shell-closed cluster, which also shows higher melting temperature than the geometrically closed-shell system of Na_{55}. The strong correlation between connectivity of bonds and melting temperature is also seen in the case of Ga (Ref. 10) and Al clusters.[14] Thus, we conclude that electronic structure affect its melting behavior strongly. We believe that it is possible to verify the prediction of the present work experimentally with the calorimetry method.

Note added in proof. A very recent experimental report by Kostko *et al.*[15] supports our conclusion regarding the spherical nature and size of Na_{58}.

*Electronic address: mslee@unipune.ernet.in

†Electronic address: kanhere@unipune.ernet.in

[1] M. Schmidt, R. Kusche, B. von Issendorff, and H. Haberland, Nature (London) **393**, 238 (1998); R. Kusche, Th. Hippler, B. von Issendorff, and H. Haberland, Eur. Phys. J. D **9**, 1 (1999).

[2] M. Schmidt and H. Haberland, C. R. Phys. **3**, 327 (2002); H. Haberland, T. Hippler, J. Donges, O. Kostko, M. Schmidt, and B. von Issendorff, Phys. Rev. Lett. **94**, 035701 (2005).

[3] A. Aguado and J. M. López, Phys. Rev. Lett. **94**, 233401 (2005).

[4] G. A. Breaux, D. A. Hillman, C. M. Neal, R. C. Benirschke, and M. F. Jarrold, J. Am. Chem. Soc. **126**, 8628 (2004); G. A. Breaux, C. M. Neal, B. Cao, and M. F. Jarrold, Phys. Rev. Lett. **94**, 173401 (2005).

[5] K. Joshi, S. Krishnamurty, and D. G. Kanhere, Phys. Rev. Lett. **96**, 135703 (2006); S. Krishnamurty, S. Chacko, D. G. Kanhere, G. A. Breaux, C. M. Neal, and M. F. Jarrold, Phys. Rev. B **73**, 045406 (2006).

[6] Vienna *Ab initio* Simulation Package (VASP), Technishe Universität Wien, 1999.

[7] S. Chacko, D. G. Kanhere, and S. A. Blundell, Phys. Rev. B **71**, 155407 (2005).

[8] A. Vichare, D. G. Kanhere, and S. A. Blundell, Phys. Rev. B **64**, 045408 (2001); S. Krishnamurty, K. Joshi, D. G. Kanhere, and S. A. Blundell, *ibid.* **73**, 045419 (2006).

[9] G. Wrigge, M. Astruck Hoffmann, and B. v. Issendorff, Phys. Rev. A **65**, 063201 (2002).

[10] S. Krishnamurty, K. Joshi, S. Zorriasatein, and D. G. Kanhere, cond-mat/0608414 (to be published).

[11] B. Silvi and A. Savin, Nature (London) **371**, 683 (1994).

[12] M.-S. Lee, S. Chacko, and D. G. Kanhere, J. Chem. Phys. **123**, 164310 (2005).

[13] A. Rytkönen, H. Häkkinen, and M. Manninen, Phys. Rev. Lett. **80**, 3940 (1998).

[14] C. M. Neal, A. K. Starace, M. F. Jarrold, K. Joshi, S. Krishnamurty, and D. G. Kanhere (unpublished).

[15] O. Kostko, B. Huber, M. Moseler, and B. von Issendorff, Phys. Rev. Lett. **98**, 043401 (2007).